ORIGINAL SCIENTIFIC PAPER

CROATICA CHEMICA ACTA

Croat. Chem. Acta **2022**, *95*(4), 157–165
Published online: July 9, 2023
DOI: 10.5562/cca3936

HKD 1926

Ternary Coordination Compounds of Copper(II) with Glycine and 2,2'-bipyridine: Synthesis, Structural Characterization, Magnetic and Biological Properties

Darko Vušak,[1] Katarina Mišković Špoljarić,[2] Jurica Jurec,[3] Dijana Žilić,[3] Biserka Prugovečki[1,*]

[1] Division of General and Inorganic Chemistry, Department of Chemistry, Faculty of Science, University of Zagreb, Horvatovac 102a, HR-10000, Zagreb, Croatia
[2] Department of Medical Chemistry, Biochemistry and Clinical Chemistry, Faculty of Medicine, Josip Juraj Strossmayer University of Osijek, J. Huttlera 4, HR-31000 Osijek, Croatia
[3] Laboratory for Magnetic Resonances, Division of Physical Chemistry, Ruđer Bošković Institute, Bijenička cesta 54, HR-10000 Zagreb, Croatia
* Corresponding author's e-mail address: biserka@chem.pmf.hr

RECEIVED: November 3, 2022 * REVISED: March 9, 2023 * ACCEPTED: March 15, 2023

THIS PAPER IS DEDICATED TO PROF. BRANKO KAITNER ON THE OCCASION OF HIS 80TH BIRTHDAY

Abstract: Three new coordination compounds of copper(II) with glycine (HGly) and 2,2'-bipyridine (bipy) were synthesized by solution-based and mechanochemical methods: $[Cu(Gly)(H_2O)(bipy)][Cu(Gly)(SO_4)(bipy)]\cdot 6H_2O$ (**1a·6H₂O**), $[Cu(Gly)(H_2O)(bipy)]_2SO_4$ (**1b**), $[Cu(Gly)(H_2O)(bipy)]_2SO_4\cdot H_2O$ (**1b·H₂O**). The amount of water in the reaction mixture influenced the product of crystallization. All compounds were characterized by X-ray diffraction methods and form 1D infinite chains or 2D sheets of complex ions connected by π-interactions. Compounds **1a·6H₂O** and **1b** were characterized by X-band electron spin resonance (ESR) spectroscopy and the values of **g**-tensors for Cu(II) ions were determined. Compounds **1a·6H₂O** and **1b** showed pronounced antiproliferative activity toward a panel of six human cell lines. The most impared was HepG2 cell line at 10^{-5} mol dm^{-3} concentration (74.5 % reduction of cell growth) followed by moderate activity toward KATO III, Caco-2, MDA-MB-231, PANC-1 and MRC-5 cells at 10^{-4} mol dm^{-3} concentration of compounds **1a·6H₂O** and **1b**. Generally, both compounds express similar antiproliferative effect on evaluated cells.

Keywords: X-ray diffraction, ESR spectroscopy, crystallization, mechanochemistry, ternary coordination compounds, copper(II), glycine, carcinoma, tumor cell lines.

INTRODUCTION

COPPER is an essential trace metal ion in our body and is the key element for the regular function of many proteins (cytochrome *c* oxidase, plastocyanin, ceruloplasmin, dopamine-monooxygenase, tyrosinase, superoxide dismutase (SOD)).[1,2] Defects in copper homeostasis lead to human diseases (Wilson's and Menkes disease). The first copper(II) complexes with amino acid were prepared in 1841 and scientists' interest in these compounds continued in the 20th century.[3] Ternary coordination compounds of copper(II) with amino acids and heterocyclic bases have been investigated for decades mostly due to their pronounced antitumor activity.[4–7] Investigations by different research groups showed that the mode of their action against tumor cells was DNA cleavage via reactive oxygen species generation, mitochondrial toxicity, or direct interaction with DNA.[8–12] Ternary coordination compounds of copper with amino acids and heterocyclic bases have been also investigated as model compounds in the study of copper interactions with DNA/proteins.[13–15] Also, recently this group of coordination compounds has been investigated for the purpose of developing new materials with certain magnetic properties, chemical sensors, and the potential of storing solvents or other molecules.[7,15] Three crystal structures containing copper(II), 2,2'-bipyridine and

glycinate are published in Cambridge Structural Database (CSD),[16] containing different anions (chloride, nitrate or polyoxomolybdate). In all three reported crystal structures geometry around the copper(II) atom is a distorted square pyramid, where 2,2'-bipyridine and glycinate ligands form chelate rings with copper(II) atom in the equatorial plane, while solvent molecule (water or DMF) or chloride ion are coordinated in the apical position.[17–20]

As a part of our ongoing research on ternary copper(II) coordination compounds with amino acids/amino acid derivatives and heterocyclic bases [6,21–23], we explored the versatility of intermolecular interactions and structure-property relationship in ternary coordination compounds of copper(II) with glycine (HGly) and 2,2'-bipyridine (bipy). We have performed solution-based and liquid-assisted mechanochemical reactions of copper(II) sulfate with glycine and 2,2'-bipyridine. The effects of different copper(II) sulfates (hydrated and anhydrous) and solvent (water and methanol) on crystallization and crystal structures were investigated. The following new compounds were obtained: $[Cu(Gly)(H_2O)(bipy)][Cu(Gly)(SO_4)(bipy)]\cdot 6H_2O$ (**1a·6H$_2$O**), $[Cu(Gly)(H_2O)(bipy)]_2SO_4$ (**1b**), $[Cu(Gly)(H_2O)(bipy)]_2SO_4\cdot H_2O$ (**1b·H$_2$O**).

Considering that there were an estimated 19.2 million newly diagnosed cancer cases and 9.9 million cancer deaths in 2020,[24] it is important to find more effective and selective, economical options to combat against cancer. Since synthesized compounds (**1a·6H$_2$O**, **1b**, **1b·H$_2$O**) contain copper(II) in combination with amino acid, such compounds have proven to be useful in the therapeutic direction making them suitable as antitumor drugs.[25] Knowing the potential of copper(II) complexes we tested the biological potential of synthesized compounds as antitumor remedies.

EXPERIMENTAL

Materials and methods

All chemicals for syntheses were obtained from commercial sources (Gram-Mol, Carlo Erba, Acros, Scharlau, Alfa Aesar) and were used without further purification. Grinding experiments were performed on Retch MM200 vibrational mixing mill operating at a frequency of 25 Hz, using Teflon jars (V = 14 mL) with one stainless steel ball (diameter 8 mm). All chemicals used for cell cultivation and bioassay were manufactured by Sigma-Aldrich, MERCK.

Solution-based Syntheses

Synthesis of $[Cu(Gly)(H_2O)(bipy)][Cu(Gly)(SO_4)(bipy)]\cdot 6H_2O$ (1a·6H$_2$O)

Copper(II) hydroxide (24.4 mg, 0.25 mmol), copper(II) sulfate pentahydrate (62.4 mg, 0.25 mmol), 2,2'-bipyridine (78.1 mg, 0.5 mmol) and glycine (37.5 mg, 0.5 mmol) were dissolved in 10.0 mL of water. The resulting mixture was heated for 15 minutes at boiling point and then filtered. Dark blue prisms, suitable for single-crystal X-ray diffraction analysis, crystallized from the mother liquor. Crystals gradually decompose outside the mother liquor.

Synthesis of $[Cu(Gly)(H_2O)(bipy)]_2SO_4\cdot H_2O$ (1b·H$_2$O)

Copper(II) hydroxide (24.4 mg, 0.25 mmol), copper(II) sulfate pentahydrate (62.9 mg, 0.25 mmol), 2,2'-bipyridine (78.1 mg, 0.5 mmol) and glycine (37.5 mg, 0.5 mmol) were dissolved in 10.0 mL of methanol. The resulting mixture was heated for 15 minutes at boiling point and filtered. Dark blue prisms of **1b·H$_2$O**, suitable for single-crystal X-ray diffraction analysis, crystallized from the mother liquor. Crystals are stable outside of the mother liquor. Along with **1b·H$_2$O**, blue crystals of $[Cu(\mu\text{-}SO_4)(H_2O)_2(bipy)]$ (CSD refcode: ABPZCU)[26] crystallize from the solution.

Synthesis of $[Cu(Gly)(H_2O)(bipy)]_2SO_4$ (1b)

Copper(II) hydroxide (24.4 mg, 0.25 mmol), anhydrous copper(II) sulfate (39.9 mg, 0.25 mmol), 2,2'-bipyridine (78.1 mg, 0.5 mmol) and glycine (37.5 mg, 0.5 mmol) were dissolved in 10.0 mL of methanol. The resulting mixture was heated for 15 minutes at boiling point and filtered. Dark blue prisms, suitable for single-crystal X-ray diffraction analysis, crystallized from the mother liquor. Crystals are stable outside the mother liquor.

Liquid-assisted Mechanochemical Syntheses

Synthesis of $[Cu(Gly)(H_2O)(bipy)][Cu(Gly)(SO_4)(bipy)]\cdot 6H_2O$ (1a·6H$_2$O)

Copper(II) hydroxide (24.4 mg, 0.25 mmol), anhydrous copper(II) sulfate (39.9 mg, 0.25 mmol), 2,2'-bipyridine (78.1 mg, 0.5 mmol) and glycine (37.5 mg, 0.5 mmol) were placed into a milling jar and water was added (36 µL, 2 mmol; η = 0.2 µL mg^{-1}). Grinding was performed for 15 minutes. The product was analysed by powder X-ray diffraction and the pattern was consistent with the powder pattern calculated from the crystal structure of **1a·6H$_2$O** (Scheme 2).

Synthesis of $[Cu(Gly)(H_2O)(bipy)]_2SO_4\cdot H_2O$ (1b·H$_2$O)

Copper(II) hydroxide (24.4 mg, 0.25 mmol), copper(II) sulfate pentahydrate (62.4 mg, 0.25 mmol), 2,2'-bipyridine (78.1 mg, 0.5 mmol) and glycine (37.5 mg, 0.5 mmol) were placed into a milling jar and methanol was added (40 µL, 1 mmol; η = 0.2 µL mg^{-1}). Grinding was performed for 15 minutes. The product was analysed by powder X-ray diffraction and the pattern was consistent with the powder pattern calculated from crystal structures of **1b·H$_2$O** and $[Cu(\mu\text{-}SO_4)(H_2O)_2(bipy)]$, but the diffraction pattern also contained several diffraction maxima of unidentified phases (Scheme 2).

Synthesis of $[Cu(Gly)(H_2O)(bipy)]_2SO_4$ (1b)

Copper(II) hydroxide (24.4 mg, 0.25 mmol), anhydrous copper(II) sulfate (39.9 mg, 0.25 mmol), 2,2'-bipyridine (78.1 mg, 0.5 mmol) and glycine (37.5 mg, 0.5 mmol) were placed into a milling jar and methanol was added (40 µL, 1.0 mmol; η = 0.2 µL mg^{-1}). Grinding was performed for 15 minutes. The product was analysed by powder X-ray diffraction and the pattern was consistent with the powder pattern calculated from the crystal structure of **1b** (Scheme 2).

X-ray Diffraction Methods

Single-crystal X-ray diffraction data of **1a·6H₂O**, **1b·H₂O** and **1b** were measured on an Oxford Diffraction Xcalibur3 CCD diffractometer with MoK_α radiation (λ = 0.71073 Å). Crystals of **1a·6H₂O** decompose outside of the mother liquor so a single-crystal was placed into a capillary transparent to X-ray radiation for data collection. Diffraction data were processed in CrysAlisPRO program package.[27] Crystal structures were solved and refined in WinGX software.[28] The crystal structure of **1a·6H₂O** was solved by SHELXT,[29] and crystal structures of **1b·H₂O** and **1b** were solved by SHELXS[30] program. All structures were refined using full-matrix least-squares refinement based on F^2 against all reflections in SHELXL program.[31] All non-hydrogen atoms were refined anisotropically. Hydrogen atoms were placed in calculated positions (aromatic hydrogen atoms) or in positions found in the Fourier difference map. Hydrogen atoms belonging to all water molecules were constrained to O–H and H···H distances to 0.85(1) Å and 1.39(2) Å, respectively. The sulfate ion in **1b** is disordered in two positions since the two-fold axis passes through the sulfur atom and occupancies of oxygen atoms were restrained to 0.5. Geometry parameters of crystal structures were calculated using PLATON.[32] Visualizations of crystal structures were made using Mercury 2021.3.0.[33] Crystal structures of **1b**, **1a·6H₂O**, **1b·H₂O** are deposited in Cambridge Structural Database under numbers 2217105–2217107, respectively.

X-ray powder diffraction data were measured at room temperature on a Panalytical AERIS diffractometer in a Bragg-Brentano geometry using CuK_α radiation (λ = 1.54184 Å). Measurements were performed in 2θ range 5 – 40° with a step size 0.022° and measurement time per step 15.045 s. The data were analysed using Highscore Software Suite.[34]

X-band Electron Spin Resonance (ESR) Spectroscopy

Bruker Elexsys 580 FT/CW ESR spectrometer was used to investigate complexes **1a·6H₂O** and **1b**. The measurements have been performed at liquid nitrogen temperature, 78 K, and at room temperature, 298 K. During the ESR measurements the microwave frequency was 9.71 ± 0.01 GHz at the liquid nitrogen temperature and 9.63 ± 0.01 GHz for the measurements at room temperature. In all measurements, magnetic field modulation amplitude was set to 0.5 mT and modulation frequency to 100 kHz.

In vitro Assay of Biological Activity

1a·6H₂O and **1b** were prepared in sterilized water as a stock solution at the 10^{-2} mol dm^{-3} concentration. Prior to application into the bioassay compounds were diluted in a cell culture medium to obtain working concentration as follows: 10^{-3}; 10^{-4}; 10^{-5} and 10^{-6} mol dm^{-3}.

Cell Cultivation

Bioactivity of compounds **1a·6H₂O** and **1b** were evaluated on a panel of six human cells lines: MRC-5 (normal fibroblasts; ATCC CCL-171); Caco-2 (colorectal adenocarcinoma; ATCC HTB-37); KATO III (gastric carcinoma; ATCC HTB-103); PANC-1 (pancreatic carcinoma; ATCC CRL-1469); Hep-G2 (hepatocellular carcinoma; ATCC HB-8065,); MDA-MB 231 (mammary adenocarcinoma; ATCC CRM-HTB-26). Cells were cultivated in the Dulbecco Modified Eagle medium (DMEM) with the addition of 10 % fetal bovine serum, 2 mmol dm^{-3} glutamine and 1 % of non-essential amino acids in a CO_2 incubator (IGO 150 CELLlife TM, JOUAN, ThermoFisher Scientific, Waltham, MA, USA) until they reach 85 % of confluence. Cultivation was set under a predetermined condition of 5 % CO_2 and 37 °C. For further manipulation cells were detached from the growth surface with 0.25 % trypsin/EDTA. The viability of cells was identified by 0.2 % erythrosine B solution under the light microscope (Axiovert 25, Carls Zeiss, Jena, Germany).

Bioassay – MTT test

Antiproliferative effects of compounds **1a·6H₂O** and **1b** were determined by 3-(4,5-dimethylthiazol-2-yl)-2,5-diphenyltetrazolium bromide (MTT) assay.[35] Cells were seeded in 96 micro well flat bottom plates (Greiner, Frickenhausen, Austria) at a concentration of 2 × 10^4 cells mL^{-1} and left overnight in the CO_2 incubator allowing them to attach to the plate surface. 24 hours later, investigated compounds were added and left to act for the next 72 hours. On the fifth day of the test, the medium was discarded and 5 mg mL^{-1} of MTT was added. After 4 hours of incubation at 37 °C water-insoluble MTT-formazan crystals were dissolved in DMSO. Absorbance was measured at 595 nm on the Elisa microplate reader (iMark, BIORAD, Hercules, CA, USA). Control cells were grown under the same conditions. Blank represents medium without cells containing MTT. All experiments were performed at least three times in triplicates. The percentage of viable cells was calculated by the following equation:

$$(A_{sample} - A_{background}) / (A_{control} - A_{background}) \times 100\ (\%).$$

From obtained results, we calculated the concentration of compounds **1a·6H₂O** and **1b** leading to a reduction of viable cells by 50 %. The parameter was designated as IC_{50} and applied for comparison among investigated compounds (**1a·6H₂O**; **1b**).

STATISTICA 14.0.0.15 (TIBCO Software Inc. Tulsa, USA)[36] was used for statistical analysis of the results of biological activity. Results are expressed as the mean value of triplicates (±) standard deviation (SD). Mann-Whitney U test and student t-test were applied for data analysis. Differences were considered statistically significant at $p < 0.05$.

RESULTS AND DISCUSSION

Synthesis

Two approaches were used for the syntheses of different solvates of ternary copper(II) coordination compounds with glycine (HGly) and 2,2'-bipyridine (bipy) – solution-based syntheses and liquid-assisted grinding (LAG). In solution-based syntheses, two different copper(II) sulfates (anhydrous and pentahydrate) were used, 2,2'-bipyridine, glycine and copper(II) hydroxide as well as two different solvents – water and methanol (Scheme 1). In an aqueous solution, with copper(II) sulfate pentahydrate pure crystals of $[Cu(Gly)(H_2O)(bipy)][Cu(SO_4)(Gly)(bipy)]\cdot 6H_2O$ (**1a·6H₂O**) were obtained. When water was replaced with methanol, with the same reactants, less hydrated $[Cu(Gly)(H_2O)(bipy)]_2SO_4\cdot H_2O$ (**1b·H₂O**) crystallized, but in a mixture with $[Cu(\mu\text{-}SO_4)(H_2O)_2(bipy)]$ (CSD refcode: ABPZCU). By replacing copper(II) sulfate pentahydrate with anhydrous copper(II) sulfate we obtained $[Cu(Gly)(H_2O)(bipy)]_2SO_4$ (**1b**) in methanol solution.

In LAG synthesis we used different copper(II) sulfates (pentahydrate and anhydrous) to control the amount of water in the system. All three compounds (**1a·6H₂O**, **1b·H₂O** and **1b**) were obtained, but **1b·H₂O** crystallized along with $[Cu(\mu\text{-}SO_4)(H_2O)_2(bipy)]$. In the diffraction pattern of **1b·H₂O** there are also some unidentified diffraction maxima that cannot be attributed to either reactants or other hydrates described in this paper. Due to weak intensities and only few maxima we could not identify this impurity phase. Powder diffraction patterns of the reaction products compared with calculated diffraction patterns from crystal structures are given in Scheme 2.

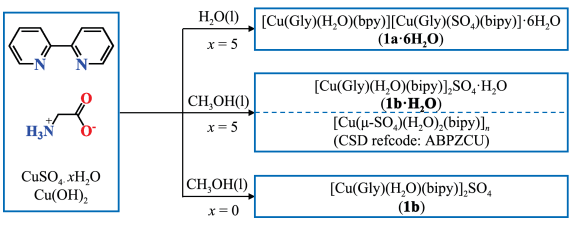

Scheme 1. Solution-based syntheses of compounds **1a·6H₂O**, **1b·H₂O** and **1b**.

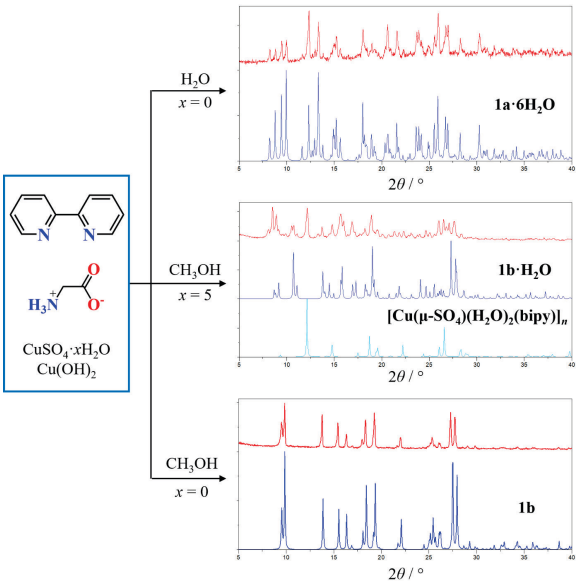

Scheme 2. Liquid-assisted mechanochemical syntheses (LAG) of compounds **1a·6H₂O**, **1b·H₂O** and **1b**. Powder patterns with a red line are experimental powder patterns of products of LAG reactions, while powder patterns with a blue line are calculated from corresponding crystal structures.

Crystal Structures

Crystallographic data for **1a·6H₂O**, **1b·H₂O** and **1b** are given in Table S1. ORTEP drawings with atom labelling scheme of all compounds are given in Figure S1. The formula unit of compounds **1b·H₂O** and **1b** contains two complex cations $[Cu(Gly)(H_2O)(bipy)]^+$ and one sulfate anion. In both compounds copper(II) ion is pentacoordinated by one *N,N'*-donating bipyridine ligand and one *N,O*-donating glycinate ligand in the basal plane and an apically coordinated water molecule (Figure 1, Table S2). The asymmetric unit of coordination compound **1b·H₂O** additionally contains one water molecule of crystalization per formula unit. In **1a·6H₂O**, the asymmetric unit contains the same complex cation $[Cu(Gly)(H_2O)(bipy)]^+$, complex anion $[Cu(Gly)(SO_4)(bipy)]^-$ and six water molecules of crystallization. In complex anion, the copper(II) ion is also pentacoordinated with one 2,2'-bipyridine and one glycinate in the basal plane but with apically coordinated sulfate anion (Figure 1, Table S2). In **1a·6H₂O** geometry of both complex cation and anion can be described as square-pyramidal with additional close contact of the oxygen atom. The carboxylate group of one complex cation is in close contact with a copper atom of the neighboring complex cation (Cu–O distance is 2.975(2) Å), while the water molecule of crystallization is

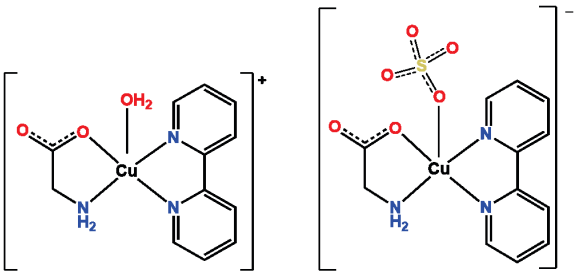

Figure 1. Schematic representation of complex cations and anions in **1a·6H$_2$O**, **1b·H$_2$O** and **1b**.

close to the copper atom of a complex anion (Cu–O distance is 3.245(3) Å). Consequently, apical Cu–O bonds in **1a·6H$_2$O** are longer (2.3589(17) and 2.608(2) Å) than apical bonds in **1b·H$_2$O** and **1b** (2.2429(15) – 2.2809(14) Å) indicating *trans*-influence in **1a·6H$_2$O**. Also, complex cations [Cu(Gly)(H$_2$O)(bipy)]$^+$ in **1a·6H$_2$O** have more distorted geometry than other complex cations in other two structures, due to hydrogen bonding of coordinated water molecule with sulfate ion in neighboring complex anion (Figures 3 and S2).

Due to asymmetrical coordination in equatorial plane, there are two possible isomers of complex species, considering apically coordinated oxygen atom. Since all described crystal structures are centrosymmetric, racemic mixtures of all isomers are present in crystal structures.

In all three compounds, complex species are π-stacked (Figure 2) forming 1D chains or 2D layers. In **1a·6H$_2$O** complex anions form 2D layers (Figure S3) with centroid–centroid (Cg–Cg) distances 3.7456(16)–4.3577(16) Å, while complex cations form dimers (closest Cg–Cg distance is 3.6557(13) Å) which form 1D chains (with Cg–Cg distances between dimers 5.3303(13)–5.9498(14) Å). Only 1D chains of π-stacked complex cations are present in **1b·H$_2$O** (Cg–Cg distances 3.5590(12)–4.1008(14) Å) and **1b** (Cg–Cg distances 3.5435(12)–4.0381(14) Å).

Extensive hydrogen bonding is present in all crystal structures. All amino group hydrogen atoms, except one belonging to complex cation in **1a·6H$_2$O**, form hydrogen bonds with sulfate ions (d(N–H···O$_{sulfate}$) = 2.752(4) – 3.002(4) Å). In **1b·H$_2$O** and **1b** sulfate ions act as a bridge between π-stacked chains of complex species (Figures 3a and b, Table S3). In **1b** sulfate ions are disordered in two positions of equal occupancy (two-fold axis is passing through sulfur atom) and sulfate in both positions form equivalent hydrogen bonds (Figure 3a). In **1a·6H$_2$O** amino group of complex cations [Cu(Gly)(H$_2$O)(bipy)]$^+$ is also hydrogen-bonded to sulfate ion in [Cu(Gly)(SO$_4$)(bipy)]$^-$ by one hydrogen atom, and both amino group hydrogen atoms in complex anions form intra- or intermolecular hydrogen bonds with sulfate ions (Figure 3c). Five out of six crystallization water molecules are interconnected through

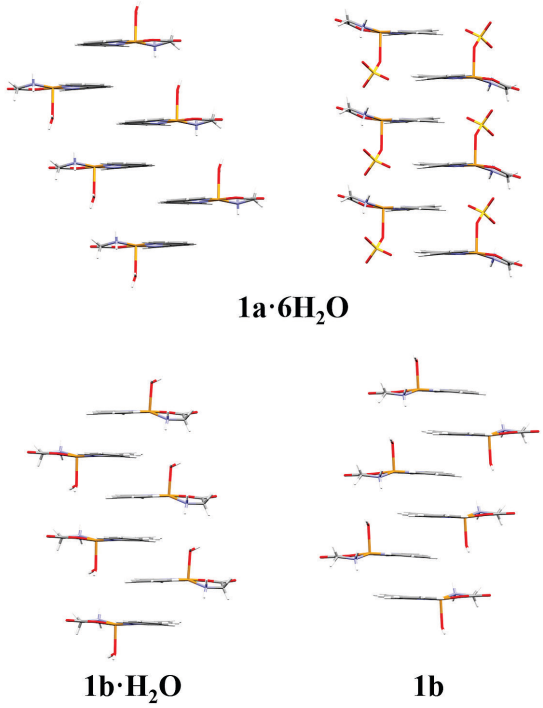

Figure 2. π-stacking of complex species in compounds **1a·6H$_2$O** (complex cations left, anions right), **1b·H$_2$O** and **1b**.

hydrogen bonds along *c*-axis and connect layers of complex cations and anions (Figure S3). The sixth crystallization water molecule is in a discrete pocket and connects complex cations.

X-band Electron Spin Resonance (ESR) Spectroscopy

Compounds **1a·6H$_2$O** and **1b** were investigated by X-band electron paramagnetic resonance (EPR) or electron spin resonance (ESR) spectroscopy. The representative spectra, obtained at room temperature and liquid nitrogen temperature are shown in Figure 4. For the spectral simulations we used EasySpin software[37] with the following form of the spin-Hamiltonian for copper(II) ions:[38,39]

$$\mathbf{H} = \mu_B \cdot \mathbf{B} \cdot \mathbf{g} \cdot \mathbf{S}. \quad (1)$$

In Eq. (1) μ_B is Bohr magneton, **g** is the **g**-tensor, **B** is the magnetic field and **S** is the electron spin operator. For all simulations, hyperfine interaction i.e. the interaction between electron and nuclear spins, was omitted because it was not experimentally observed. In the spectral simulations, the same values of **g**-tensors were used at both investigated temperatures. The spectra were simulated allowing the line width of the assumed Lorentzian lineshape to change with temperature. The spin-Hamiltonian values obtained from the simulations are given in Table 1.

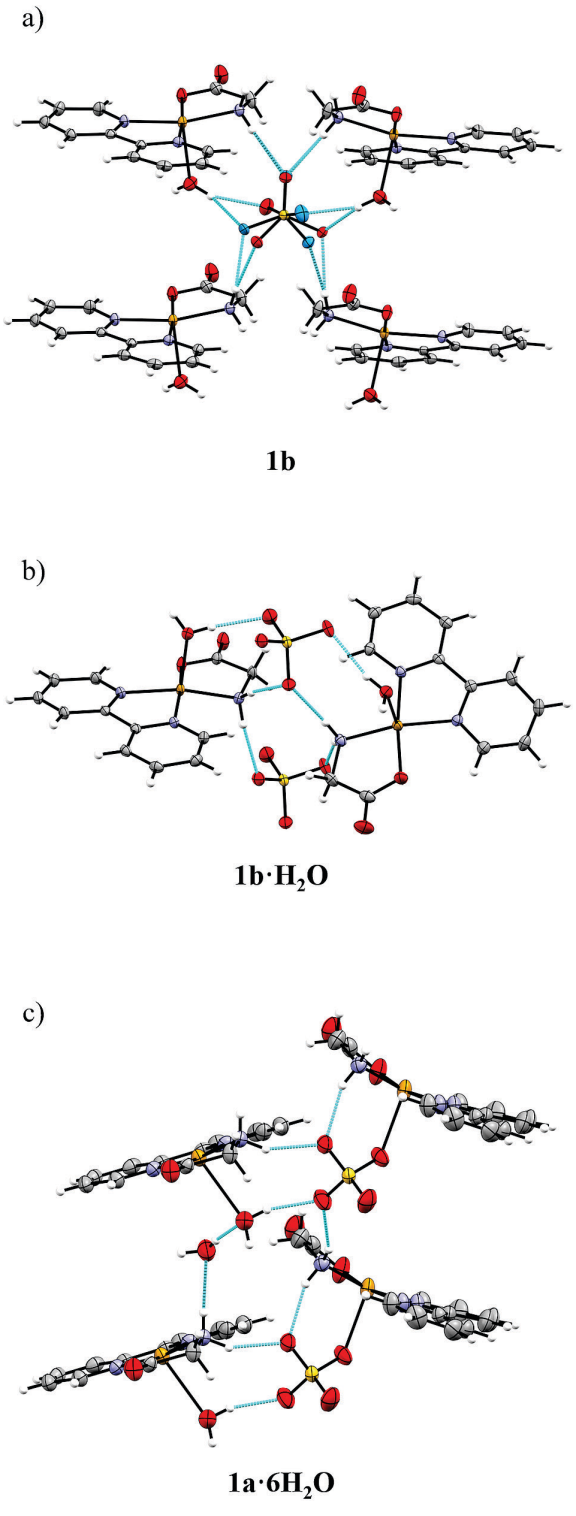

Figure 3. Hydrogen bonds involved with sulfate ion in: a) **1b**, b) **1b·H₂O** and c) **1a·6H₂O**. Oxygen atoms in two disordered positions in **1b** are marked with red and blue colors.

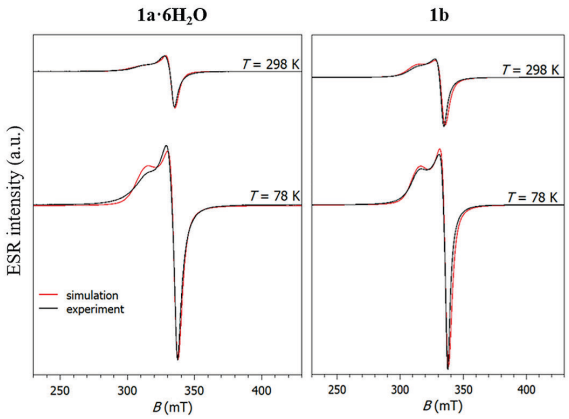

Figure 4. Experimental (black lines) and simulated (red lines) ESR spectra of polycrystalline samples of the investigated complexes **1a·6H₂O** and **1b** at 78 K and at 298 K. The ESR intensities of the spectra at different temperatures are presented in the real ratios.

The small variations in the local geometry of Cu(II) coordination can cause the distribution of g_x–, g_y– and g_z– values around some average values.[40] This effect described by $\mathbf{g}_{strain}$ parameters is also considered in the simulations with the values presented in Table 1. The obtained *g*-values are in agreement with the literature data.[41] Obtained values $g_x \approx g_y < g_z$ are expected for the elongated octahedral, square pyramidal or square planar copper geometry.[42] This is in agreement with structurally determined distorted square pyramidal geometries in these compounds. In the case of **1a·6H₂O,** there are two copper(II) ions in the asymmetric unit, but due to mutually similar copper geometries and *g*-parameters, only one ESR line is observed in powder spectra. The distance between the two nearest copper atoms is 5.333 Å and 5.142 Å for **1a·6H₂O** and **1b**, respectively. The Cu–Cu distances are large enough for significant exchange interactions to be observed in these compounds.

Anticancer Activity

Bio evaluation of compounds **1a·6H₂O** and **1b** against a panel of five human malignant cell lines opposite normal MRC-5 fibroblast point to a very similar pathway of activity of both compounds. Panel of evaluated cell lines was chosen with the intent to estimate the potential targeting tissue of evaluated compounds since all malignant cell lines originated from the most diagnosed cancers in the world [24]. Notably impaired by the presence of compounds **1a·6H₂O** and **1b** were Caco-2, PANC-1 and KATO III, followed by MDA-MB 231, Hep-G2 and MRC-5 (Figure S4). The most illustrious concentration was 10^{-4} mol dm^{-3} on the

Table 1. The principal *g*-values obtained from the ESR spectral simulations, together with the parameter used for the simulations: $\mathbf{g}_{strain}$ and linewidths l_w.

Compounds	$\mathbf{g} = [g_x\ g_y\ g_z]$	$\mathbf{g}_{strain}$	l_w / mT	T / K
1a·6H₂O	[2.07 2.07 2.22]	[0.02 0.08 0.09] [0.03 0.12 0.16]	4.37 2.67	78 298
1b	[2.06 2.06 2.21]	[0.11 0.02 0.08] [0.02 0.08 0.09]	3.88 4.65	78 298

Table 2. IC_{50} concentration of compounds **1a·6H₂O** and **1b**.

	IC_{50} / μM					
	MDA-MB 231	Hep-G2	KATO III	PANC-1	Caco-2	MRC-5
1a·6H₂O	21.0 (1.1)	5.1 (1.1)#	12.4 (1.2)*	19.0 (2.1)	11.0 (0.3)*	40.4 (1.9)
1b	24.6 (1.7)	5.1 (0.8)#	11.1 (1.8)*	10.4 (2.1)*	10.2 (1.1)*	37.2 (2.8)

Mean (SD) of three independent experiments (± SD); student t-test (*$p < 0.05$; #$p < 0.01$) compared to MRC-5.

evaluated cell panel. Cell growth of named cell lines was suppressed from 94.9 % (Caco-2) up to 79.8 % (MRC-5) indicating significant antiproliferative activity ($p < 0.05$) of compounds **1a·6H₂O** and **1b**. Hep-G2 was the most sensitive to the presence of evaluated compounds which was seen by the high impact of 10^{-5} mol dm^{-3} concentration which reduce cell growth by 74.5 %. Gained results of the MTT bioassay provide insight into the antiproliferative activity of synthesized compounds and allow us to appraise inhibitory concentration which reduces cell growth by 50 % (IC_{50}). Results indicate selective influence on different cell lines with spare effect on normal human fibroblasts (IC_{50} = 37.2; 40.4 μM). Malignant cancer cell lines express higher sensitivity towards **1a·6H₂O** and **1b** compounds what is visible from IC_{50} values (Table 2).

CONCLUSIONS

We have shown that by controlling the amount of solvent and the selection of reactants – it is possible to obtain different ternary copper(II) coordination compound with 2,2'-bipyridine and glycine. In a controlled manner by reactions in solution as well as in the solid state we obtained two hydrates ($[Cu(Gly)(H_2O)(bipy)][Cu(SO_4)(Gly)(bipy)]\cdot 6H_2O$ (**1a·6H₂O**), $[Cu(Gly)(H_2O)(bipy)]_2SO_4\cdot H_2O$ (**1b·H₂O**)) and one anhydrous coordination compound ($[Cu(Gly)(H_2O)(bipy)]_2SO_4$ (**1b**)). Even when a low amount of water was present in the reaction mixture in methanolic solution, an aqua complex was formed (**1b**), showing a high preference of those ternary compounds towards water. Although crystals of **1a·6H₂O** decompose in the air at room temperature we were able to obtain a pure compound in mechanochemical synthesis indicating that the compound is stable under reaction conditions (high relative humidity). **1b·H₂O** was not obtained pure, it crystallized with $[Cu(\mu\text{-}SO_4)(H_2O)_2(bipy)]$ in solution-based and solid-state synthesis. Compounds with less water content **1b·H₂O** and **1b** have some similarities in their structure, they both contain the same building units – complex cations $[Cu(Gly)(H_2O)(bipy)]^+$ and sulfate ions. Both structures have similar packing of complex cations by π-interactions into infinite 1D chains. **1a·6H₂O** on the other hand contains complex cations $[Cu(Gly)(H_2O)(bipy)]^+$ and complex anions $[Cu(Gly)(SO_4)(bipy)]^-$, where anions form 2D layers through π-interactions, while cations form dimers which form 1D chains. Some intermolecular interactions are conserved in all structures – the presence of π-interactions between bipyridine rings and hydrogen bonds between amino groups of glycinate and sulfate ions. From ESR simulations, *g*-values of Cu(II) ions were determined for **1a·6H₂O** and **1b** compounds, which is in the agreement with copper square-pyramidal geometries. Although compounds **1a·6H₂O** and **1b** vary in the preparation process (water/methanol solution) from a biological point of view they act very similarly on chosen cell lines. Since both compounds indicate a significant antiproliferative effect on malignant cancer cells with a spare effect on normal cell line we can conclude that these two compounds have the potential for further biological evaluation.

Acknowledgment. The research was supported by the Croatian Science Foundation under the projects HRZZ-IP-2018-01-3168 and IP-2018-01-1227.

Supplementary Information. Supporting information to the paper is attached to the electronic version of the article at: https://doi.org/10.5562/cca3936.

PDF files with attached documents are best viewed with Adobe Acrobat Reader which is free and can be downloaded from Adobe's web site.

REFERENCES

[1] R. A. Festa, D. J. Thiele, *Curr Biol.* **2011**, *21(21)*, 877–883. https://doi.org/10.1016/j.cub.2011.09.040

[2] M. C. Linder, *Biochemistry of copper; Series: Biochemistry of the Elements, Vol. 10*, Springer Science+Business Media, New York, **1991**. https://doi.org/10.1007/978-1-4757-9432-8

[3] J.-B. Boussingault, *Ann. Chim. Phys.* **1841**, *3*, 257.

[4] L. Ruiz-Azuara, M. E. Bravo-Gómez, *Curr. Med. Chem.* **2010**, *17*, 3606–3615. https://doi.org/10.2174/092986710793213751

[5] C. Santini, M. Pellei, V. Gandin, M. Porchia, F. Tisato, C. Marzano, *Chem. Rev.* **2014**, *114*, 815–862. https://doi.org/10.1021/cr400135x

[6] D. Vušak, B. Prugovečki, D. Milić, M. Marković, I. Petković, M. Kralj, D. Matković-Čalogović, *Cryst. Growth Des.* **2017**, *17*, 6049–6061. https://doi.org/10.1021/acs.cgd.7b01157

[7] A. Wojciechowska, A. Szuster-Ciesielska, M. Sztandera, R. Bregier-Jarzębowska, A. Jarząb, T. Rojek, U. K. Komarnicka, A. Bojarska-Junak, J. Jezierska, *Appl. Organomet. Chem*. **2020**, *34*, e5698. https://doi.org/10.1002/aoc.5698

[8] A. I. Valencia-Cruz, L. I. Uribe-Figueroa, R. Galindo-Murillo, K. B. López, A. G. Gutiérrez, A. Vázquez-Aguirre, L. Ruiz-Azuara, E. Hernández-Lemus, C. Mejía C, *PLoS ONE* **2013**, *8(1)*, e54664. https://doi.org/10.1371/journal.pone.0054664

[9] A. G. Gutiérrez, A. Vázquez-Aguirre, J. C. García-Ramos, M. Flores-Alamo, E. Hernández-Lemus, L. Ruiz-Azuara, C. Mejía, *J. Inorg. Biochem.* **2013**, *126*, 17–25. https://doi.org/10.1016/j.jinorgbio.2013.05.001

[10] L. Becco, J. C. García-Ramos, L. Ruiz Azuara, D. Gambino, B. Garat, *Biol. Trace Elem. Res.* **2014**, *161*, 210–215. https://doi.org/10.1007/s12011-014-0098-1

[11] M. E. Bravo-Gomez, J. C. Garcia-Ramos, I. Gracia-Mora, L. J. Ruiz-Azuara, *Inorg. Biochem*. **2009**, *103*, 299–309. https://doi.org/10.1016/j.jinorgbio.2008.10.006

[12] R. Galindo-Murillo, J. Hernandez-Lima, M. Gonzalez-Rendon, F. Cortes-Guzman, L. Ruiz-Azuara, R. Moreno-Esparza, *Phys. Chem. Chem. Phys.* **2011**, *13*, 14510–14515. https://doi.org/10.1039/c1cp20183b

[13] X. Y. Le, S. Liao, X. P. Liu, X. L. Feng, *J. Coord. Chem.* **2006**, *59*, 985–995. https://doi.org/10.1080/00958970500443144

[14] S. R. Liao, X. Y. Le, X. L. Feng, *J. Coord. Chem.* **2008**, *61*, 847–856. https://doi.org/10.1080/00958970701476943

[15] N. D. Corona-Motolinia, B. Martínez-Valencia, L. Noriega, B. L. Sánchez-Gaytán, A. Mendoza, F. J. Meléndez-Bustamante, M. E. Castro, E. González-Vergara, *Metals* **2021**, *11*, 1541. https://doi.org/10.3390/met11101541

[16] C. R. Groom, I. J. Bruno, M. P. Lightfoot, S. C. Ward, *Acta Crystallogr*. **2016**, *B72*, 171–179. https://doi.org/10.1107/S2052520616003954

[17] C. J. Neitzel, R. Desiderato, *Cryst. Struct. Commun.* **1975**, *4*, 333–336.

[18] M. Yodoshi, M. Odoko, N. Okabe, *Acta Cryst.* **2005**, *E61*, m2299–m2301. https://doi.org/10.1107/S1600536805032265

[19] J. C. García-Ramos, R. Gallindo-Murillo, A. Tovar-Tovar, A. L. Alonso-Saenz, V. Gómez-Vidales, M. Flores-Álamo, L. Ortiz-Frade, F. Cortes-Guzmán, R. Moreno-Esparza, A. Campero, L. Ruiz-Azuara, *Chem. Eur. J*. **2014**, *20*, 13730–13741. https://doi.org/10.1002/chem.201402775

[20] H. Liu, Y. Zhang, D. Yu, *Acta Cryst.* **2008**, *E64*, m305–m307. https://doi.org/10.1107/S0108270108023585

[21] D. Vušak, B. Prugovečki, D. Matković-Čalogović, *Acta Crystallogr. A* **2018**, *74*, E338. https://doi.org/10.1107/S2053273318090125

[22] D. Vušak, K. Ležaić, J. Jurec, D. Žilić, B. Prugovečki, *Heliyon* **2022**, *8*, e09556. https://doi.org/10.1016/j.heliyon.2022.e09556

[23] B. Prugovečki, D. Vušak, K. Ležaić, M. Jurković, *Acta Crystallogr. A* **2021**, *77*, C975. https://doi.org/10.1107/S0108767321087250

[24] https://gco.iarc.fr/today/fact-sheets-cancers. Date accessed: 28/10/2022

[25] B. Martínez-Valencia, N. D. Corona-Motolinia, E. Sánchez-Lara, B. L. Sánchez-Gaytán, M. Cerro-López, A. Mendoza, M. E. Castro, F. J. Meléndez-Bustamante, E. González-Vergara, *Crystals* **2020**, *10*, 492. https://doi.org/10.3390/cryst10060492

[26] J. C.Tedenac, N. Dinh Phung, C. Avinens, M. Maurin, *J. Inorg. Nucl. Chem*. **1976**, *38*, 85–89. https://doi.org/10.1016/0022-1902(76)80055-3

[27] CrysAlisPRO (version 171.42.63a), Rigaku Oxford Diffraction, Yarnton, UK, 2022.

[28] L. J. Farrugia, *J. Appl. Cryst.* **2012**, *45*, 849–854. https://doi.org/10.1107/S0021889812029111

[29] G. M. Sheldrick, *Acta Crystallogr., Sect. A: Found. Adv*. **2015**, *A71*, 3–8. https://doi.org/10.1107/S2053273314026370

[30] G. M. Sheldrick, *Acta Crystallogr., Sect. A: Found. Crystallogr.* **2008**, *64*, 112–122. https://doi.org/10.1107/S0108767307043930

[31] G.M. Sheldrick, *Acta Crystallogr., Sect. C: Struct. Chem*. **2015**, *C71*, 3–8. https://doi.org/10.1107/S2053229614024218

[32] A. L. Spek, *J. Appl. Cryst*. **2003**, *36*, 7–13. https://doi.org/10.1107/S0021889802022112
[33] C. F. Macrae, I. Sovago, S. J. Cottrell, P. T. A. Galek, P. McCabe, E. Pidcock, M. Platings, G. P. Shields, J. S. Stevens, M. Towler, P. A. Wood, *J. Appl. Cryst*. **2020**, *53*, 226–235. https://doi.org/10.1107/S1600576719014092
[34] T. Degen, M. Sadki, E. Bron, U. König, G. Nénert, *Powder Diffr*. **2014**, *29*, S13–S18. https://doi.org/10.1017/S0885715614000840
[35] T. Mossman, *J. Immunol. Methods* **1983**, *65*, 55–63. https://doi.org/10.1016/0022-1759(83)90303-4
[36] https://docs.tibco.com/products/tibco-statistica-all-servers-14-0-1. Date accessed: 28/10/2022
[37] S. Stoll, A. Schweiger, *J. Magn. Reson*. **2006**, *178*, 42–55. https://doi.org/10.1016/j.jmr.2005.08.013
[38] O. Kahn, *Molecular Magnetism*, Wiley-VCH Inc., New York, 1993.
[39] A. Carrington, A. D. McLachlan, *Introduction to Magnetic Resonance*, Harper and Row, New York, 1967.
[40] B. Szymańska, D. Skrzypek, D. Kovala-Demertzi, M. Staninska, M. A. Demertzis, *Spectrochim. Acta A* **2006**, *63*, 518–523. https://doi.org/10.1016/j.saa.2005.05.038
[41] M. Chikira, C. Hee Ng, M. Palaniandavar, *Int. J. Mol. Sci*. **2015**, *16*, 22754–22780. https://doi.org/10.3390/ijms160922754
[42] E. Garribba, G. Micera, *J. Chem. Educ*. **2006**, *83*, 1229. https://doi.org/10.1021/ed083p1229